UNIVERSITY OF BIRMINGHAM

Research at Birmingham

Tool Temperature in Slotting of CFRP Composites

El-Hofy, Mohamed; Soo, Sein; Aspinwall, David; Sim, W. M.; Pearson, D.; M'Saoubi, R.; Harden, Peter

Link to publication on Research at Birmingham portal

45th SME North American Manufacturing Research Conference, NAMRC 45, LA, USA

Tool temperature in slotting of CFRP composites

M.H. El-Hofy[a,1], S.L. Soo[a,*], D.K. Aspinwall[a], W.M. Sim[b], D. Pearson[c], R. M'Saoubi[c], P. Harden[a]

[a]Machining Research Group, Department of Mechanical Engineering, School of Engineering, University of Birmingham, Edgbaston, Birmingham, B15 2TT, UK
[b]Airbus Operations Ltd., Pegasus House, Aerospace Avenue, Filton, Bristol, BS34 7PA, UK
[c]Seco Tools (UK) Ltd., Alcester, B49 6EL, UK

Abstract

Following a brief review on the effects of process parameters on cutting temperatures and associated workpiece integrity when machining carbon fibre reinforced plastic (CFRP) composites, the paper details experimental work to assess tool temperature regimes and machinability when slot milling CFRP. This involved variation in workpiece lay-up, tool geometry, cutting environment and operating levels. Typically, cutting temperatures varied between ~180-350°C with fibres orientated at 0° and 45° producing the highest temperatures and cutting forces. Worn tooling and dry cutting also produced less favourable results. Increasing cutting speed from 200 to 350 m/min caused a rise in temperature by an average of ~25% while increasing feed rate from 0.03 to 0.06 mm/tooth produced a reduction of ~18%.

Keywords: Slotting; milling; CFRP; temperature

* Corresponding author. Tel.: +44-121-414-4196; fax: +44-121-414-4201.
  E-mail address: s.l.soo@bham.ac.uk

[1] Currently at Advanced Manufacturing Research Centre (AMRC) with Boeing, University of Sheffield, Advanced Manufacturing Park, Wallis Way, Catcliffe, Rotherham, S60 5TZ, UK.

1. Introduction

The use of carbon fibre reinforced plastic (CFRP) composites in aerospace applications such as primary and secondary aircraft structures has increased rapidly over the last decade. Such lightweight composites possess good physical and mechanical properties including superior corrosion resistance, high specific strength/stiffness and good dimensional stability, with the possibility of making complex shapes [1]. The net result is reduced fuel consumption and environmental impact for aircraft such as the Airbus A350 XWB or Boeing 787 Dreamliner, which utilise around 50% carbon fibre composite structures. A characteristic of parts made from composites is that they are produced to near-net-shape, which necessitates further trimming to reach the desired product configuration.

When machining, the majority of cutting power is converted to heat [2]. Due to the lower thermal conductivity of CFRP, ~50% of the cutting temperature is absorbed by the tool, compared to 18% when machining metallic materials [3]. Owing to the brittle nature of chips and the intermittent cutting action of processes such as end milling/routing, heat absorption by the chip is low [4]. A key measure in assessing damage threshold is the rise in temperature beyond Tg, which is defined as the transition between the rubbery and glassy state of the binder phase which normally ranges from 180-270°C for epoxy based composites [5]. Controlling the heat generated at the cutting zone is the key requirement to produce "first-time right" parts in order to avoid the high cost of part rejection [6, 7] and as a consequence, there is a need to measure and understand the factors affecting temperature. In composite machining, unlike some metals, it is not easy to tell the cutting temperature from chip colour as indicated by oxidisation [8]. Temperature can be measured by resistance, use of infra-red (IR) cameras, thermocouples or other devices [9], however their appropriateness is subject to the complexity of the machining process such as whether the tool rotates as in milling or is obscured during operation as in drilling. In the case of slot milling where the actual cutting action is obscured and interrupted with short periods of heating and cooling, dependent on the cutting edge/flute arrangements, the use of IR cameras is not ideal [10]. In such cases, implanting thermocouples in the workpiece [5, 11-13] has been extensively used. Leaving aside fabrication time/costs and equipment requirements, one of the main shortcomings of using thermocouples especially if implanted in the tool, lies in signal delays and reduced sensitivity which are dependent on sensor location relative to the heat source and the mass of the tool, as detailed by Kerrigan et al.[14]. Additionally, the difference between surface and the internal tool temperature is a further consideration [8]. Experimental work and finite element modelling by Kerrigan and O'Donnell [15] using a wireless thermocouple system in edge trimming of CFRP addressed this aspect.

The effect of cutting parameters such as cutting speed on cutting temperature has been reported by many researchers [5, 10, 11, 14] as has feed rate [14, 16, 17] and depth of cut. Rahman et al. [18] found that a critical cutting speed V_{cr}, initiated temperatures beyond Tg. Other factors such as matrix content or resin percentage, layup configuration and tool material, were also found to alter the cutting temperature as reported by Inoue et al. [19]. Fibres also affect cutting temperature [20, 21], for example, Merino-Pérez et al. [11] found that when drilling CFRP, the cross-linking density and degree of crystallinity of fibres affected fibre flexibility and hence temperature. Other factors such as workpiece thickness, fibre orientation and workpiece overhang in edge trimming [10, 14], also influence temperature as does tool wear [22]. In terms of tool geometry, Wurtz et al. [23] reported that decreasing secondary clearance of the tool adversely affected interface friction, while increased tool diameter raised the heat capacity of the tool. The majority of the published milling work addressing temperature measurement has studied the edge trimming operation, however for processes such as slotting of CFRP, the results are not comparable especially if low cutting speeds are employed. Ucar and Wang [13] recorded temperatures of up to 44°C at 35 m/min when end milling CFRP and up to 330°C at 132 m/min in other work by Wang et al. [5]. When shallow face milling, Ghafarizadeh et al. [10] found that fibre orientation affected the cutting force and cutting temperature.

The use of emulsion coolant was reported by Mondelin et al. [24] to reduce the coefficient of friction between diamond and CFRP from 0.06 to 0.02 during dry and lubricated cutting, however, for aerospace applications, the use of liquid based coolants can present problems due to absorption concerns. Dry cutting or use of air cooling together with strong extraction is preferred. The application of refrigerants such as nitrogen [16] or carbon dioxide [25] has been reported, but freon used by Colligan and Ramulu [26] is no longer an environmentally friendly option. Chilled air (CA) of -30°C [27] or a mixture of chilled/refrigerated air and oil mist (CAMQL) [28], have been shown to be effective in reducing tool wear and surface roughness. Recently, Jia et al. [12] used nitrogen gas (down to -50°C) and found that the low temperature enhanced workpiece surface roughness by changing the fibre breaking plane angle if

applied at high pressure and flow rate, but no quantitative values of pressure or flow rate were presented. Cutting temperature not only plays a role in tool life and workpiece quality, but it can also affect dust particle size and concentration in the air, which can have adverse effects on health as reported by Haddad et al. [29].

2. Experimental work and procedures

The majority of trials utilised multi-directional CFRP laminates comprising 3 different lay-up arrangements of pre-preg layers (0.26 mm thick), having fibre orientations of 0˚, 45˚, 90˚ and 135˚, which are denoted as Type-1, Type-2 and Type-3. The pre-pregs consisted of intermediate modulus (294 GPa) carbon fibres with an epoxy resin matrix. Additionally, a small number of panels were produced involving unidirectional laminates laid up in the 0˚, 45˚, 90˚ or 135˚ directions. The material designation was TORAY 3911/34%/UD268/T800SC-24K, which relates to resin type, resin content by weight (%), fibre areal weight (g/m^2) and fibre type. Both Type-1 and Type-3 panels were each made up of 40 plies and stacked according to the sequence $[45˚/0˚/135˚/90˚]_{5S}$ and $[45˚/0˚/135˚/135˚/135˚/90˚/45˚/45˚/45˚/0˚/135˚/135˚/90˚/45˚/45˚/0˚/135˚/135˚/90˚/45˚]_S$ respectively (total thickness of 10.4 mm), while Type-2 laminates involved 36 plies arranged according to $[45˚/0˚/135˚/0˚/90˚/0˚/135˚/0˚/45˚]_{2S}$, with a post cure thickness of 9.36 mm. The final panel dimensions were 600 x 550 x 10.4/9.36 mm. Autoclave cured laminates were then sectioned into 2 different sized coupons typically 100 x 100 mm for force/temperature measurement and slot quality analysis and 260 x 240 mm for extended machining trials. Three different 12 mm diameter solid carbide tools/routers with fabricated polycrystalline diamond (PCD) cutting edges and 3 flutes were used having rake and relief angles of 0˚ and 18˚ respectively, but with different helix angles of -3˚ (Tool A), 0˚ (Tool B) and 3˚ (Tool C). The PCD diamond grain size ranged up to ~30 µm.

Milling experiments were carried out on a Matsuura FX5, 3-axis CNC machining centre having a maximum rotational speed of 20,000 rpm. The coupons for cutting force/temperature/surface integrity evaluation were clamped to a Kistler 9257 platform dynamometer using a specially designed jig, while tool life coupons were held on a vacuum fixture to maximise cut length. The majority of tests involved full immersion slotting, however a 3/4 engagement strategy was also employed for tool life assessment, in which the router was operated in a raster fashion, resulting in up/down milling on consecutive passes. Kistler 5011 charge amplifiers were used with a Nicolet Sigma-60 oscilloscope for signal manipulation, with forces taken mid-slot. A stream of chilled air was generated from a vortex tube system with the chilled air directed to the cutting zone through adjustable hoses, either in a twin-nozzle or single-nozzle arrangement. Air temperatures detailed in Table 1 were measured using a thermometer placed directly after and at ~10 mm from the nozzle exit. The machining setup and difference between full immersion slotting and 3/4 engagement are shown in Fig. 1.

Table 1. Chilled air conditions in single and twin-nozzle arrangements.

Chilled air mode	Air speed* (*m/s*)	Air temperature** (˚C)		Output pressure (*bar*)
		10 mm from nozzle	At nozzle edge	
Single-nozzle	29	2	-3	0.72
Twin-nozzle	17	5	0	0.40

*Measured using an Extech AN200 anemometer at 10 mm distance from nozzle

**Measured using a thermometer

Tool flank wear was measured in accordance with ISO-8688-2, using a Wild toolmaker's microscope equipped with a Canon EOS400D digital camera. Three dimensional surface roughness parameters (Sa, St) and topography maps were obtained using an Alicona Infinite-Focus non-contact optical scanning system at 10X magnification with 159 nm vertical and 3.91 µm lateral resolutions respectively, over an area 1.5 x 5 mm. A dust extraction system evacuated particles down to 0.3 µm.
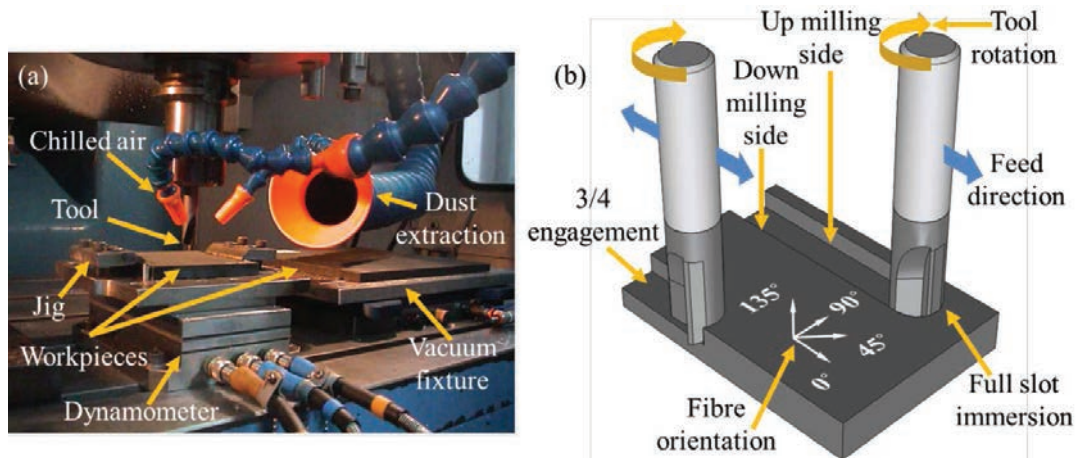
Fig. 1. (a) Milling setup on Matsuura FX5; (b) Full immersion slotting vs. 3/4 engagement strategy.

Tool temperature measurement was carried out using a wireless telemetry system from ACTARUS SAS connected to a K-type thermocouple implanted adjacent to the cutting edge (~0.5 mm) of the PCD blank. Further details of a similar tooling arrangement and system operation can be found in the paper by Kerrigan et al. [14]. Temperature (in the form of voltage signals) was measured by the thermocouple system and displayed on a Microtel K-1 digital readout unit with data subsequently relayed to and recorded (simultaneously with cutting force traces) using a Nicolet Sigma-60 oscilloscope, see Fig. 2. The thermocouple was calibrated to 0.01V for every 1˚C prior to the start of testing. In the present work, no attempt was made to calculate the actual cutting edge temperature with respect to values measured at the thermocouple location. Consequently, reported temperatures are relative and below the actual cutting zone temperature, however the difference was anticipated to be small due to the high thermal conductivity of the PCD layer (~ 600 W/mK). Peak temperatures were captured at the end of each slot.
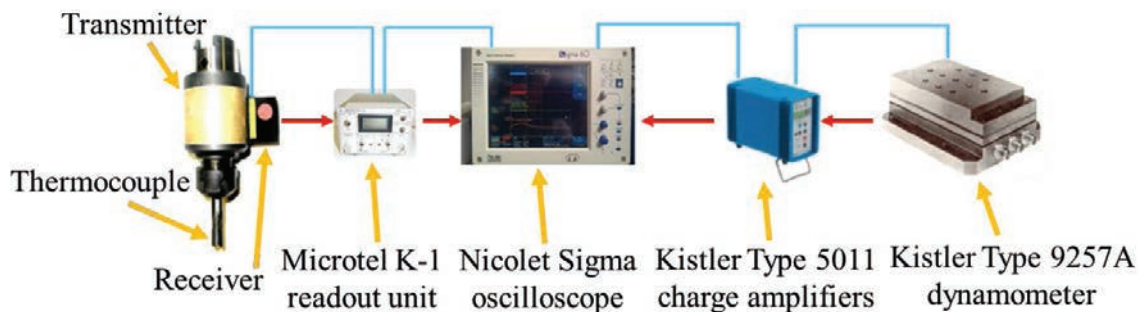

Fig. 2. Arrangement for simultaneous force and temperature signal capture using Sigma-60 oscilloscope.

The different phases of testing are detailed in Table 2 and used both new and partially worn (~ 0.1 mm flank wear) tools. Phase 1 work used new tools to cut full immersion 100 mm slots for measurement of temperature, force and workpiece topography (on the down milling side of the slot wall) followed by life tests at 3/4 engagement strategy, based on a flank wear criterion (VB) of 0.1 mm. At selected intervals during the tool life tests, the cutter was moved back to a coupon on the dynamometer and 100 mm full immersion slots were machined for force and temperature measurements. In subsequent phases (2, 3 and 4), partially worn tools (0.1 mm flank wear) were utilised and involved full immersion slotting of 100 mm length coupons only. Due to restrictions on tooling and workpiece materials, all tests were only performed once.

Table 2. Phases of testing and corresponding operating parameters / conditions.

Cutting speed (*m/min*)	Slot depth (*mm*)	Feed rate (*mm/tooth*)	Tool type	Cutting environment	Workpiece lay-up configuration
Phase 1: Effect of tool helix angle – full immersion slotting (new tools) followed by 3/4 engagement life trials to flank wear criterion VB of 0.1 mm.					
200	5	0.03	Tool A Tool B Tool C	Twin-nozzle CA	Type-1
Phase 2: Effect of workpiece lay-up configuration – full immersion slotting (partially worn tools)					
200	5	0.03	Tool A Tool B Tool C	Twin-nozzle CA	MD (Type-1 Type-2 & Type-3); UD (0˚,45˚,90˚ & 135˚)
Phase 3: Effect of cutting speed and feed rate –full immersion slotting (partially worn tools)					
200 350	5	0.03 0.06	Tool B	Twin-nozzle CA	Type-1
Phase 4: Effect of cutting environment – full immersion slotting (partially worn tools)					
200	5	0.03	Tool A Tool B	Dry Single-nozzle CA Twin-nozzle CA	Type-3

3. Results and discussion

3.1. Phase 1 tests

The temperatures recorded when using new tools during 100 mm slotting was in the region of 200˚C, with values for Tool A, Tool B and Tool C of 193˚C, 206˚C and 197˚C respectively. The small variation in temperatures reflects the marginal difference in helix angle, the tools being commercial designs. In contrast cutting forces showed greater variation relative to the 3 geometries with the highest values for cutting force (Fx). Additionally, Tool B which entailed neutral helix gave the lowest force values both for Fx and feed force (Fy). In subsequent tool life tests, cutting with 3/4 engagement produced a cut length of ~4100 mm for the flank wear criterion VB for all tools. The similarity in wear performance between the tools reflected the consistency and extreme abrasive resistance of the PCD cutting edges together with the relatively mild cutting conditions. Temperatures logged at selected intervals (on the small coupons using full immersion slotting) up to the test criteria, mirrored flank wear progression, see Fig. 3, while Fig. 4 details both temperatures and forces at test cessation and includes new tool data for comparison. In general, temperatures increased by ~25-28% over the test duration with all 3 tools maintaining their relative differences. A measurement of tool temperature recorded during 3/4 engagement cutting was ~85% of the temperature during full immersion slotting. Typically, positive helix geometry is preferred for chip evacuation compared with negative helical geometry; however this did not appear an issue in the present work because of the small difference as well as use of the forced air environment. The reduction in cutting forces shown for the worn compared to new tools in Fig. 4(b) is a reflection of the higher temperatures generated leading to greater matrix material softening.
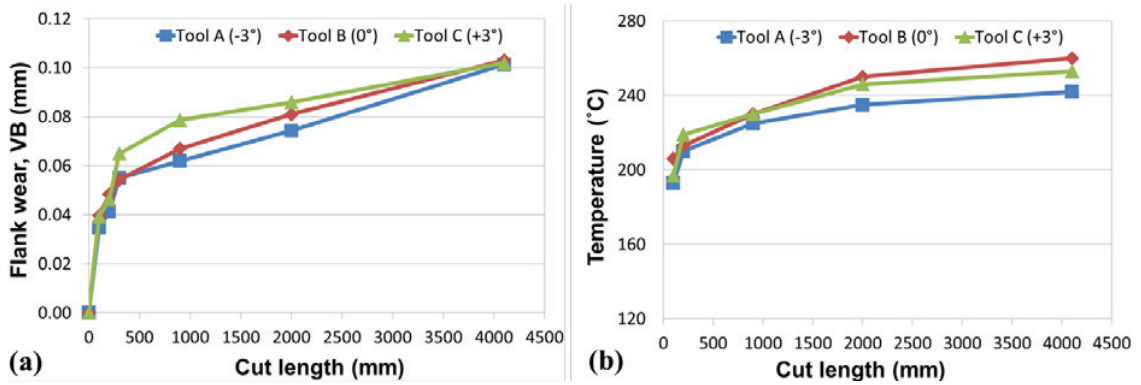
Fig. 3. (a) Tool flank wear progression; (b) Temperature variation against cut length.
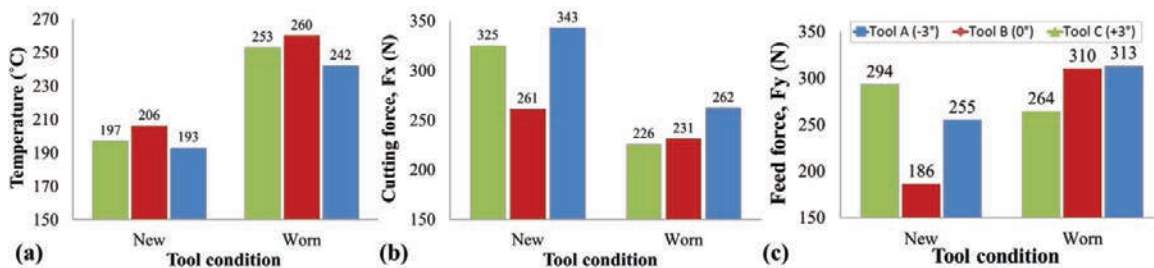

Fig. 4. (a) Temperature; (b) Cutting force, Fx; (c) Feed force, Fy using new and worn routers.

With the limited cutting associated with new tools on the first 100 mm slots, no appreciable/obvious workpiece damage was evident on either side of the slot walls. During progression of the tool life trials however, progressive damage became apparent not least due to the development of fuzzing / uncut fibres. Using Tool C (+3˚ helix angle), fuzzing occurred on the up-milled side of the slot after only a cut length of ~ 300 mm compared to 550 mm in the case of Tool B (neutral helix) and 800 mm for Tool A (-3˚ helix angle), possibly due to the positive helix geometry allowing the fibres to flex more readily and avoid cutting, as reported by Hosokawa et al. [22]. Conversely, evidence of fuzzing on the down-milled side of the slots only appeared after ~2750 mm cut length using neutral helix, compared to 3500 mm when utilising the -3˚ helix angle router, possibly due to the downward cutting action of the latter. Figure 5 details 3D topography maps of down-milled slot wall surfaces machined with new tools for each test. Plies orientated at 45˚ exhibited the most severe damage, showing considerable matrix/fibre pull-out in a repetitive pattern along the feed rate direction. The negative helix router (Tool A) produced the roughest surface of 9.94 µm Sa (200.66 µm St) with the lowest temperature recorded.

With new tool edges, cutting was dominated by shear and fracture of the fibres however with worn tools, the friction and pressure between tool and fibres would be expected to increase causing greater mechanically induced damage such as fibre and matrix pull-out. The neutral helix router produced the lowest surface roughness of 5.52 µm Sa and 89.98 µm St. Higher operating temperatures (but not to burning level) may promote smoother surfaces due to matrix softening and smearing as reported by Ghafarizadeh et al. [10]. A preferred operating temperature regime consistent with acceptable workpiece quality was discussed by Jia et al. [12].
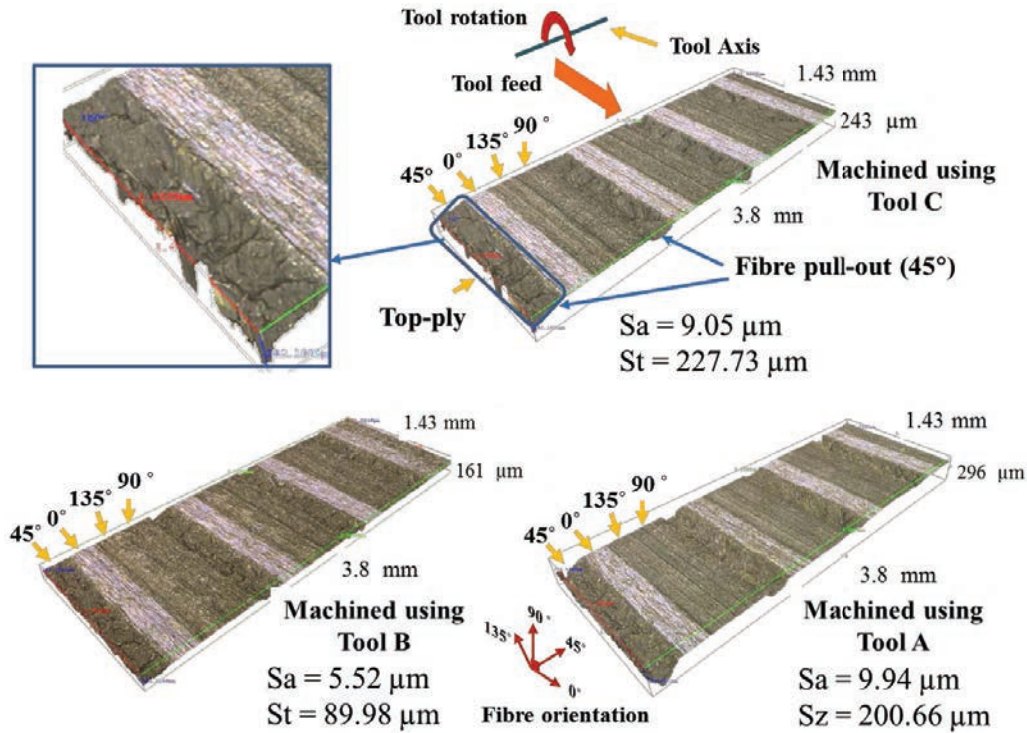
Fig. 5. Three-dimensional surface topography maps of down-milled slot wall after first slot.

3.2. Phase 2 tests

Recorded temperatures when slotting Type-1, Type-2 and Type-3 MD laminates with the 3 different routers produced similar results, Type-1 lay-up giving marginally lower values, see Fig. 6. In terms of the influence of helix angle, the temperature trends between material lay-up configuration were consistent, with Tool A producing the lowest values. Despite the markedly different lay-up configurations between the 3 types of MD laminates, with for example the Type-2 structure containing more than twice the number of 45˚ and 135˚ plies compared to 0˚ and 90˚, the difference in measured temperature did not exceed ~15˚C (between Type-1 and Type-3 using Tool A).
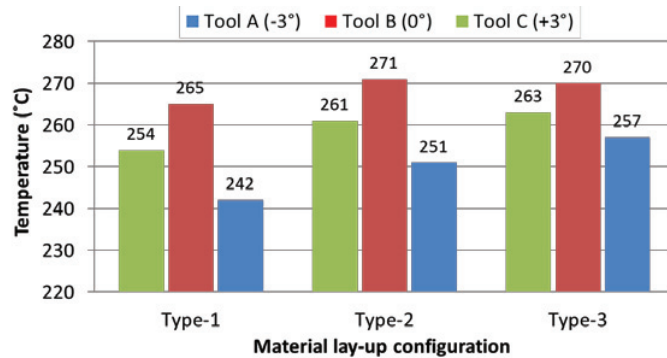

Fig. 6. Temperatures measured when slotting Type-1, Type-2 and Type-3 MD laminates with different routers.

Temperature measurements were the lowest when cutting the UD laminates orientated with fibres in the 135˚ direction, followed by laminates with 0˚ orientation irrespective of helix angle geometry, see Fig. 7. In contrast, the highest temperatures were found with fibres at 45˚, which also produced relatively high cutting forces and provides an explanation for the severity of damage observed in those layers. Ghafarizadeh et al. [10] also suggested that fibres at 45˚ were responsible for instability and dynamic forces. Cutting forces (Fx) were highest when machining 0˚ orientated UD laminates, see Fig. 8, which may have contributed to premature fracture of the PCD cutting edge in Tool C (554 N Fx and 348 N Fy) although weakening of the tool due to the implanted thermocouple could also have been a factor. Unfortunately, time constraints precluded sourcing of replacement tools.
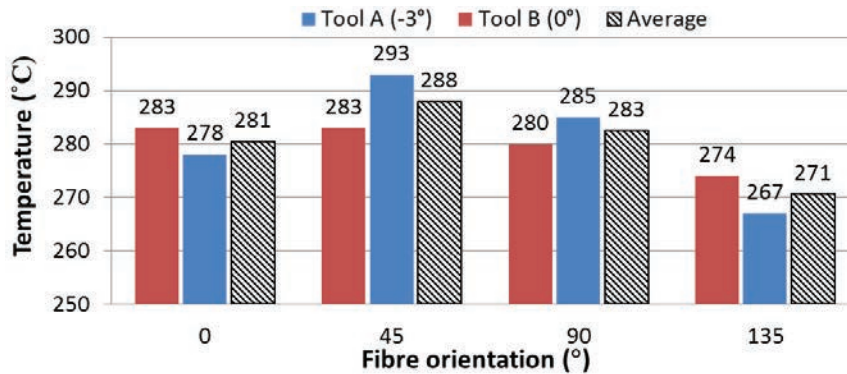

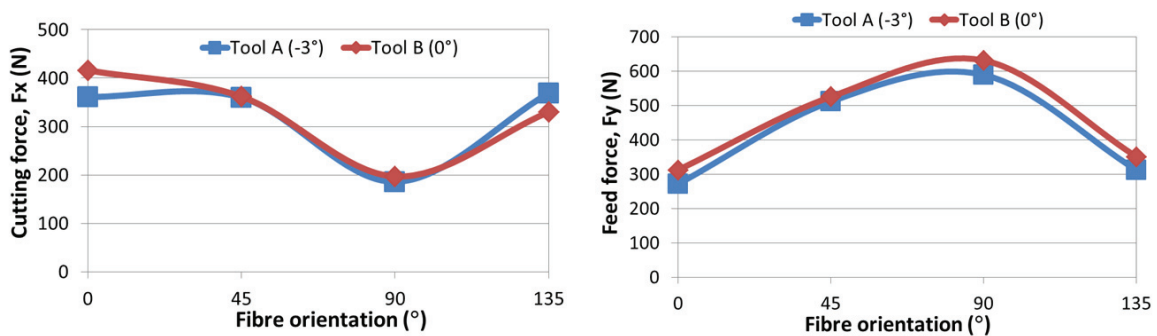Fig. 7. Temperatures measured when slotting unidirectional laminates.

Fig. 8. Forces (Fx and Fy) when slotting unidirectional laminates.

3.3. Phase 3 tests

Cutting temperature as anticipated, was found to vary with cutting speed such that higher speed generated greater temperature (average of ~25% rise in temperature as cutting speed was increased from 200 to 350 m/min) when machining with the neutral helix router (Tool B), see Fig. 9. Conversely, as feed increased (0.03 to 0.06 mm/tooth), cutting temperature reduced by ~18% at a cutting speed of 200 m/min, the fall being attributed to the lower tool-workpiece contact time. Additionally, this effect was more pronounced at the lower cutting speed level. However, it is likely that temperatures would rise with a further increase in feed rate as tool wear factors become more dominant. Although not detailed here, preliminary trials involving variation in slot depths of 1, 2 and 3 mm using Type-1 laminates produced a linear increase in cutting temperature from 70˚C to 170˚C, the linearity resulting from the repeated lay-up arrangement occurring approximately every 1 mm.
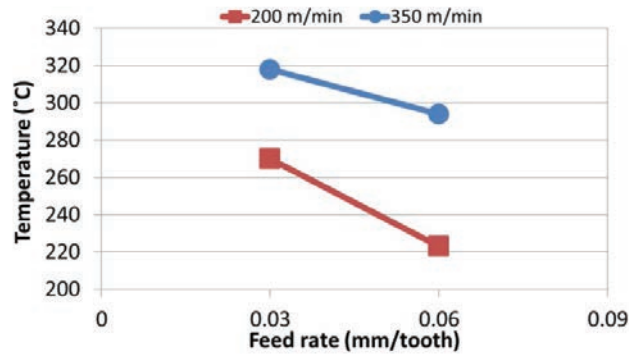
Fig. 9. Effect of cutting speed and feed rate on temperatures using neutral helix routers.

3.4. Phase 4 tests

Machining under dry conditions produced temperatures ~100˚C higher than when using chilled air, see Fig. 10(a). As highlighted in Phase 1 when using new tools, the effect of the different helix angles on temperature was negligible. More significant was the difference between the use of single or twin nozzle arrangement to deliver the chilled air, the former providing more efficient cooling (by up to ~30˚C). This was due to lower air temperature at 10 mm from the nozzle exit (~2˚C compared to ~5˚C), substantially higher air speed (~29 m/s vs. ~17 m/s) and output pressure, see Table 1. The higher air flow rate enabled quicker evacuation of CFRP dust from the cutting zone. Cutting dry led to partial melting of the epoxy matrix and burning of workpiece debris. The adverse effects of high temperatures on slotted CFRP surfaces were previously highlighted by El-Hofy et al. [30], with resin burning generally avoided when utilising chilled air operation as opposed to dry machining.

Figure 10(b) details temperature profiles for the 3 cutting environments when machining the 100 mm long slots. The rate of temperature increase during dry machining was more rapid compared to the chilled air conditions. Although not apparent, the temperature curves comprised fluctuating response corresponding to the intermittent nature of the slotting operation. In continuous slotting/machining of large workpieces, temperatures would be expected to be substantially higher (for example > 400°C in a dry environment) before reaching a plateau.
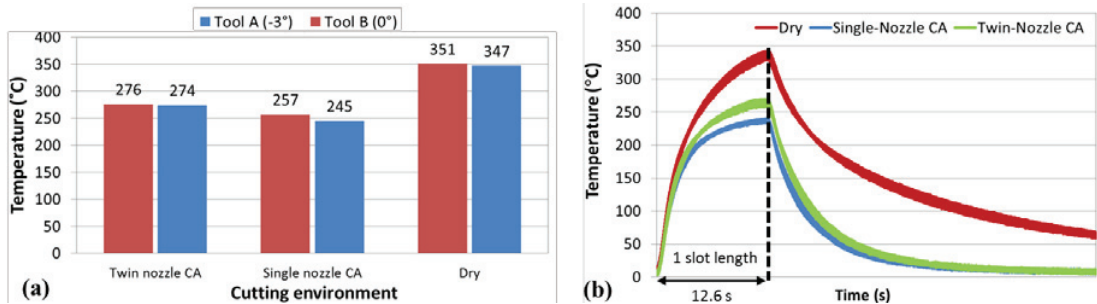

Fig. 10. (a) Temperatures for different cutting environments; (b) Sample temperature response.

4. Conclusions

Recorded tool temperatures when slotting CFRP using new and partially worn PCD routers under different environments, operating conditions, workpiece lay-up and with tools having alternative helix angles, varied between 186˚C to 351˚C. Fibres orientated at 0˚ and 45˚ produced the highest tool temperatures and cutting force, the lowest observed temperatures being associated with fibres at 135˚. Corresponding workpiece surface integrity evaluation also showed significant damage of the 45˚ plies. In the present work, the effect of differing helix angle (-3˚ to +3˚)

was somewhat marginal due to the relatively small range, but which nonetheless reflected the commercial nature of the PCD routers, selected in part for their extreme wear resistance. The difference in temperature between new and worn tools (0.1 mm VB flank wear achieved after 4100 mm cut length) when machining with chilled air delivered via a twin-nozzle arrangement was ~30%. Similarly, a significant temperature increase (~25%) was recorded when increasing cutting speed (200 to 350 m/min) however increasing feed rate reduced tool temperature due to shorter machining times. The results highlight the importance/necessity of a cooling medium when routing/slotting CFRP even when using PCD tools with their higher thermal conductivity compared to carbide.

Acknowledgements

References

[1] I. Shyha, S.L. Soo, D. Aspinwall, S. Bradley, Effect of laminate configuration and feed rate on cutting performance when drilling holes in carbon fibre reinforced plastic composites. Journal of Materials Processing Technology, 210(8) (2010) 1023-1034.

[2] M. Sato, N. Tamura, H. Tanaka, Temperature variation in the cutting tool in end milling. Journal of Manufacturing Science and Engineering, 133(2) (2011) 021005-2-021005-7.

[3] W. Konig, P. Graß, Quality definition and assessment in drilling of fibre reinforced thermosets. CIRP Annals - Manufacturing Technology, 38/1 (1989) 119-124.

[4] T. Yashiro, T. Ogawa, H. Sasahara, Cutting temperature measurement on milling process of CFRP. In Proceedings of the International Conference on Leading Edge Manufacturing in 21st century: LEM21, (2011) 3329-1-3329-4.

[5] H. Wang, J. Sun, J. Li, L. Lu, N. Li, Evaluation of cutting force and cutting temperature in milling carbon fiber-reinforced polymer composites. International Journal of Advanced Manufacturing Technology, 82(9) (2016) 1517-1525.

[6] G. Byrne, D. Dornfeld, B. Denkena, Advancing cutting technology. CIRP Annals - Manufacturing Technology, 52/2 (2003) 483-507.

[7] U. Karaguzel, M. Bakkal, E. Budak, Modeling and measurement of cutting temperatures in milling. Procedia CIRP, 46 (2016) 173-176.

[8] F.Jiang, Z. Liu, Y. Wan, Z. Shi, H. Zhang, Experimental investigation of cutting tool temperature during slot milling of AerMet 100 steel. Proceedings of the Institution of Mechanical Engineers, Part B: Journal of Engineering Manufacture, 230(5) (2015) 838-847.

[9] M.A. Davies, T. Ueda, R. M'Saoubi, B. Mullany, A.L. Cooke, On the measurement of temperature in material removal processes. CIRP Annals - Manufacturing Technology, 56/2 (2007) 581-604.

[10] S. Ghafarizadeh, , G. Lebrun, J.-F. Chatelain, Experimental investigation of the cutting temperature and surface quality during milling of unidirectional carbon fiber reinforced plastic. Journal of Composite Materials, 50(8) (2016) 1059-1071.

[11] J.L. Merino-Pérez, R. Royer, S. Ayvar-Soberanis, E. Merson, A. Hodzic, On the temperatures developed in CFRP drilling using uncoated WC-Co tools Part I: Workpiece constituents, cutting speed and heat dissipation. Composite Structures, 123 (2015) 161-168.

[12] Z. Jia, R. Fu, F. Wang, B. Qian, C. He, Temperature effects in end milling carbon fiber reinforced polymer composites. Polymer Composites, (2016) In Press.

[13] M. Ucar, Y. Wang, End-milling machinability of a carbon fiber reinforced laminated composite. Journal of Advanced Materials, 37(4) (2005) 46-52.

[14] K. Kerrigan, J. Thil, R. Hewison, G.E. O'Donnell, An integrated telemetric thermocouple sensor for process monitoring of CFRP milling operations. Procedia CIRP, 1 (2012) 449-454.

[15] K. Kerrigan, G.E. O'Donnell, Temperature measurement in CFRP milling using a wireless tool-integrated process monitoring sensor. International Journal of Automation Technology, 7(6) (2013) 742–750.

[16] W.C. Chen, Some experimental investigations in the drilling of carbon fiber-reinforced plastic (CFRP) composite laminates. International Journal of Machine Tools and Manufacture, 37(8) (1997) 1097-1108.

[17] K. Weinert, C. Kempmann, Cutting Temperatures and their effects on the machining behaviour in drilling reinforced plastic composites. Advanced Engineering Materials, 6(8) (2004) 684-689.

[18] M. Rahman, S. Ramakrishna, H.C. Thoo, Machinability study of carbon/peek composites. Machining Science and Technology, 3(1) (1999) 49-59.

[19] T. Inoue, M. Hagino, M. Matsui, L.W. Gu, Cutting characteristics of CFRP materials with end milling. Progress of Machining Technology, 407-408 (2009) 710-713.

[20] M.W. Pilling, B. Yates, M.A. Black, P. Tattersall, The thermal conductivity of carbon fibre-reinforced composites. Journal of Materials Science, 14(6) (1979) 1326-1338.

[21] E.B. Trostyanskaya, L.P. Kobets, G.M. Gunyaev, Investigation of the modulus of elasticity of carbon fibers. Polymer Mechanics, 7(5) (1971) 757-760.

[22] A. Hosokawa, N. Hirose, T. Ueda, T. Furumoto, High-quality machining of CFRP with high helix end mill. CIRP Annals - Manufacturing Technology, 63/1 (2014) 89-92.

[23] C. Wurtz, S. Rummenholler, F. Klocke, Tool design for milling process of carbon fibre reinforced plastics (CFRP). In Proceedings of the ASME 3rd Biennial Conference on Engineering System Design and Analysis (ESDA1996), (1996) 29-32.

[24] A. Mondelin, B. Furet, J. Rech, Characterisation of friction properties between a laminated carbon fibres reinforced polymer and a monocrystalline diamond under dry or lubricated conditions. Tribology International, 43(9) (2010) 1665-1673.

[25] N.W. Sorbo, J.J. Dionne, Dry drilling of stackup composite: Benefits of CO2 cooling. SAE International Journal of Aerospace, 7(1) (2014) 156-163.

[26] K. Colligan, M. Ramulu, Delamination in surface plies of graphite/epoxy caused by the edge trimming process. In Processing and manufacturing of composite materials; Proceedings of the Symposium, 112th ASME Winter Annual Meeting, Atlanta, GA, Dec. 1-6, (A93-32021 12-37), (1991) 113-125.

[27] M. Rahman, A.S. Kumar, M. Ul-Salam, M.S. Ling, Effect of chilled air on machining performance in end milling. International Journal of Advanced Manufacturing Technology, 21(10-11) (2003) 787-795.

[28] Y. Su, N. He, L. Li, A. Iqbal, M.H. Xiao, et al., Refrigerated cooling air cutting of difficult-to-cut materials. International Journal of Machine Tools and Manufacture, 47(6) (2007) 927-933.

[29] M. Haddad, R. Zitoune, F. Eyma, B. Castanie, Study of the surface defects and dust generated during trimming of CFRP: Influence of tool geometry, machining parameters and cutting speed range. Composites Part A: Applied Science and Manufacturing, 66 (2014) 142-154.

[30] M.H. El-Hofy, S.L. Soo, D.K. Aspinwall, W.M. Sim, D. Pearson, et al., Factors affecting workpiece surface integrity in slotting of CFRP. Procedia Engineering, 19 (2011) 94-99.